Highly controllable ICP etching of GaAs based materials for grating fabrication

Qiu Weibin(邱伟彬)† and Wang Jiaxian(王加贤)

College of Information Science and Engineering, Huaqiao University, Xiamen Campus, Xiamen 361021, China

Abstract: Highly controllable ICP etching of GaAs based materials with $SiCl_4$/Ar plasma is investigated. A slow etching rate of 13 nm/min was achieved with RF1 = 10 W, RF2 = 20 W and a high ratio of Ar to $SiCl_4$ flow. First order gratings with 25 nm depth and 140 nm period were fabricated with the optimal parameters. AFM analysis indicated that the RMS roughness over a 10×10 μm^2 area was 0.3 nm, which is smooth enough to regrow high quality materials for devices.

Key words: semiconductor process; inductively coupled plasma; dry etching; gratings

DOI: 10.1088/1674-4926/33/2/026001 **PACC:** 7366F; 7850G; 7855E

1. Introduction

A controllable anisotropic semiconductor dry etching process is highly desirable when fabricating electronic devices, such as heterojunction bipolar transistors (HBTs) where the mesa of the emitter and base is normally around 100 nm[1, 2]. Also, in the optical logic gates array, sampled grating with corrugation as shallow as 60 nm is critical to obtain the low coupling factors[3]. Among the numerous dry etching methods, reactive ion etching (RIE) and inductively coupled plasma (ICP) are the most popular methods[4−8]. The advantages of using ICP etching over conventional parallel plate RIE are well documented. The chamber pressure tends to be as high as 100 mTorr or more in an RIE system; conversely, ICP sources are able to operate at lower pressures 1–20 mTorr. They can also generate plasma densities a factor of 10–100 times higher than capacitive coupled discharges. As a result, these sources are capable of etching anisotropic features at etch rates comparable to or higher than conventional high-pressure RIE tools. Furthermore, large area uniformity of etching can be expected due to the low chamber pressure. In an ICP etcher, the ion energy incident on the wafer can effectively be decoupled from plasma generated by independently applying RF power to the wafer chuck. This allows the possibility of low etch-induced damage at higher etch rates. In this paper, RF1 denotes the power applied to the wafer chuck. RF1 primarily affects the ion energy. RF2 denotes the power to the source electrode coils. RF2 primarily affects the plasma density, i.e. ion flux.

$SiCl_4$ based plasma is a popular discharge for III–V materials in ICP etching[9−11]. However, most of the literature focuses on the high etching rate process, i.e. from several hundred nm to several μm per minute, with a high density plasma. In shallow grating fabrication, only tens of nm of etching depth is needed, which precludes the use of high density ICP dry etching. In order to take advantage of the benefits of the ICP method, we carried out an investigation of very low rate dry etching of GaAs based materials using $SiCl_4$/Ar at low RF power levels.

2. Experiment

100 nm of SiO_2 was deposited on a GaAs substrate with plasma enhanced chemical vapor deposition (PECVD). After that, the samples were patterned into 3, 5, 10, 20, and 30 μm wide stripes with conventional photolithography. Next, RIE with CF_4 plasma was performed to selectively remove SiO_2 and thereby transfer the patterns from the photoresist onto the SiO_2 underneath. After removing the resist, the remaining SiO_2 acted as a hard mask for ICP etching. The wafer was cleaved into small pieces in order to compare the various ICP etching treatments. All of the samples discussed in this paper were etched with a PlasmaTherm SLR 770 ICP-RIE system. Samples were transferred into the etching chamber with a load lock. An RF bias (13.56 MHz) and an inductive coil power (2 MHz) between 0–1000 W were supplied to the chamber via a primary coil in the upper electrode. The chamber pressure was maintained by a feedback controlled throttle valve. Process gases were introduced into the chamber with a series of mass flow controllers (MFCs) calibrated to flow rates as low as 0.1 sccm. The etched mesas and etching rates were characterized using a Hitachi S4800 scanning electron microscope (SEM) to provide a cross-sectional view of the cleaved strips. The 3-D pictures of the samples were measured with a Digital Instruments Dimension 3000 atomic force microscope (AFM).

3. Results and discussion

3.1. Etching properties of GaAs with various RF power levels

Figure 1 shows the etching rate and the DC bias as functions of the RF2 power for various Ar flow rates and RF1 power levels. The DC bias is the potential measured across the coil and the sample. A low DC bias is desirable since it is a measure of etch damage. The etching time was chosen to be 2 min in order to etch with a stable plasma, since the plasma is unstable and complicated for the first few seconds while it is being generated. The plasma does not ignite at extremely low RF1 power level. To solve this problem, we ignited the plasma at a higher RF1 power and then quickly switched it to the lower power level within 5 s. SEM pictures indicated that this approach did not influence the etching properties.

All of the parameters: RF1, RF2, $SiCl_4$ flow and Ar flow,

† Corresponding author. Email: wbqiu@hqu.edu.cn

Received 13 July 2011, revised manuscript received 14 August 2011

© 2012 Chinese Institute of Electronics

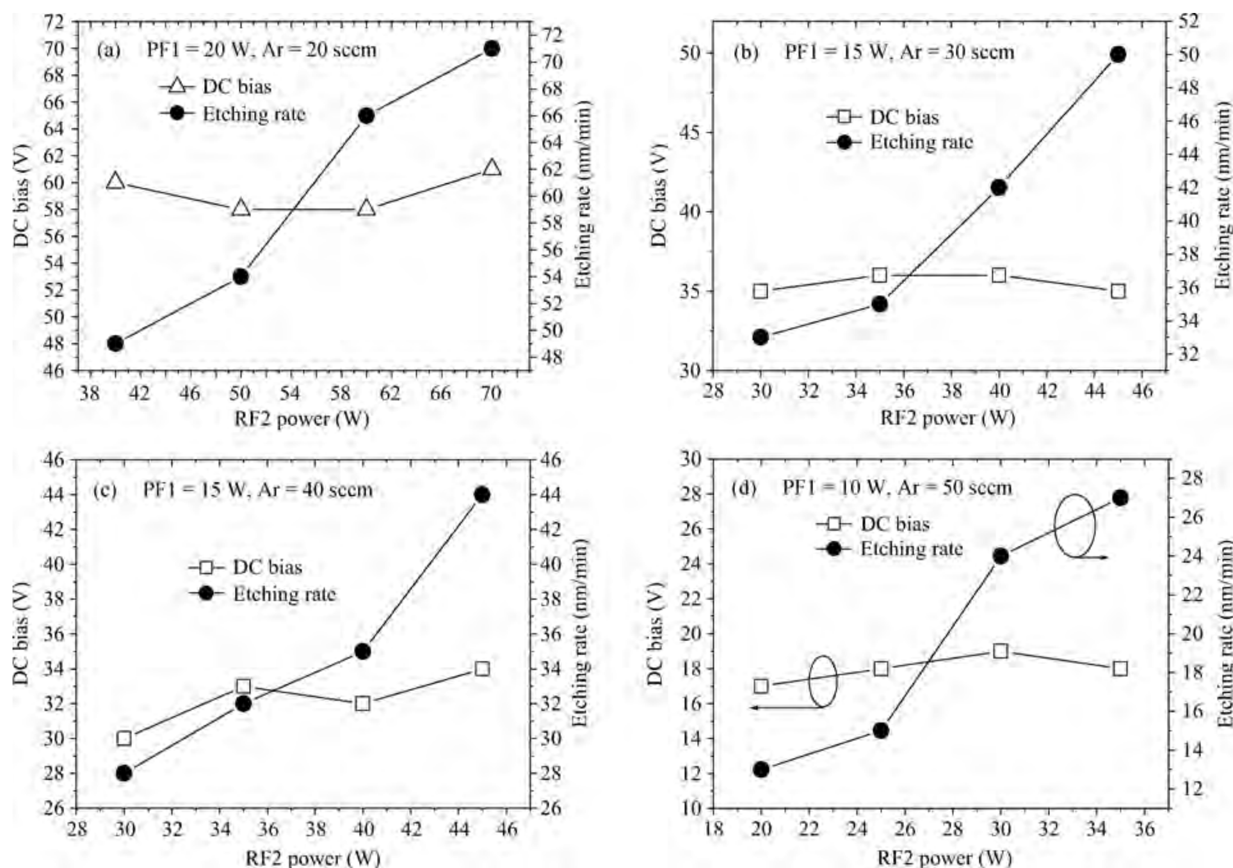

Fig. 1. Etching rate and DC bias as functions of RF2 power for different RF1 power levels and Ar flows.

can influence the etching rate. First, we fixed the $SiCl_4$ flow constant at 1 sccm and the pressure at 1 mTorr in order to ensure large area uniformity. Then, we set the Ar flow to 20 sccm, RF1 power level to 20 W, and modified the RF2 power level. One can see from Fig. 1(a) that the etching rate decreases when the RF2 power level decreases. We get to an etching rate of 48nm per minute with an RF2 power level of 40 W, but this is still not slow enough. So we decreased the RF1 power level and increased the Ar flow. An etching rate as low as 13 nm/min was obtained when the RF1 and RF2 levels were 10 and 20 W, respectively, and the Ar flow was 50 sccm.

Also from Fig. 1, we can see that the DC bias is almost constant with the same RF1 and etching gas flow. It is not modified by the RF2 power level. Furthermore, by comparing Figs. 1(b) and 1(c) we find that the DC bias did not change much as the Ar flow was changed from 30 to 40 sccm. All of these observations suggest that the DC bias is mostly determined by the RF1 power, which is attributed to generating the plasma and determines the plasma energy. One can see from the figures that the DC bias decreases with the decrease of the RF1 power level, from 60 V at 20 W RF1 power to 18 V at 10 W RF1 power. Thus, at lower RF1 power, the etch rate will be slower and damage to the surface should be reduced.

3.2. Effect of Ar flow at low RF power levels

Ar acts as a buffer gas in plasma etching, and can modify the etching profile, surface smoothness and even the etching rate[12, 13]. We kept the RF1 power at 10 W, RF2 at 20 W, pressure at 1 mTorr and increased the Ar flow from 1.3 to 50 sccm. The etching time was fixed at 2 min. The SEM pictures are shown in Fig. 2. There are two etching effects during plasma etching. One is chemical etching, which may induce undercut etching. The other is physical etching, which induces vertical etching by ion bombardment. It is evident that physical bombardment would damage the etching surface although it gives an anisotropic etch.

From the above pictures, we can see that in the low Ar flow region, where the Ar flow is less than 20 sccm, the dominant process was chemical etching. The sidewall is clearly undercut due to the Cl-based etching. When the Ar flow was increased from 20 to 34 sccm, the physical etching, where Ar acts as the buffer of the etching process, becomes more and more significant and the etching rate decreases accordingly. At the same time, the side wall becomes more vertical. When the Ar flow increases further, the physical bombardment becomes dominant and chemical etching becomes negligible due to the ultra-low $SiCl_4$ concentration. We should point out that when the Ar flow is larger than 38 sccm, the etching rate is saturated even though the Ar flow continues to increase. As shown in Fig. 3, the chamber pressure kept increasing as the total gas flow increased. This is due to the limited capability of the turbo pump in our ICP system.

The etching rate increases with increasing chamber pressure because it is harder to pump the $SiCl_4$ from the chamber when the pressure is high. This leads to an enhancement in the amount of etchant gas remaining in the chamber and also in the number of ion collisions, at higher chamber pressure[14]. Thus, the etching rate stops decreasing and begins to saturate at high

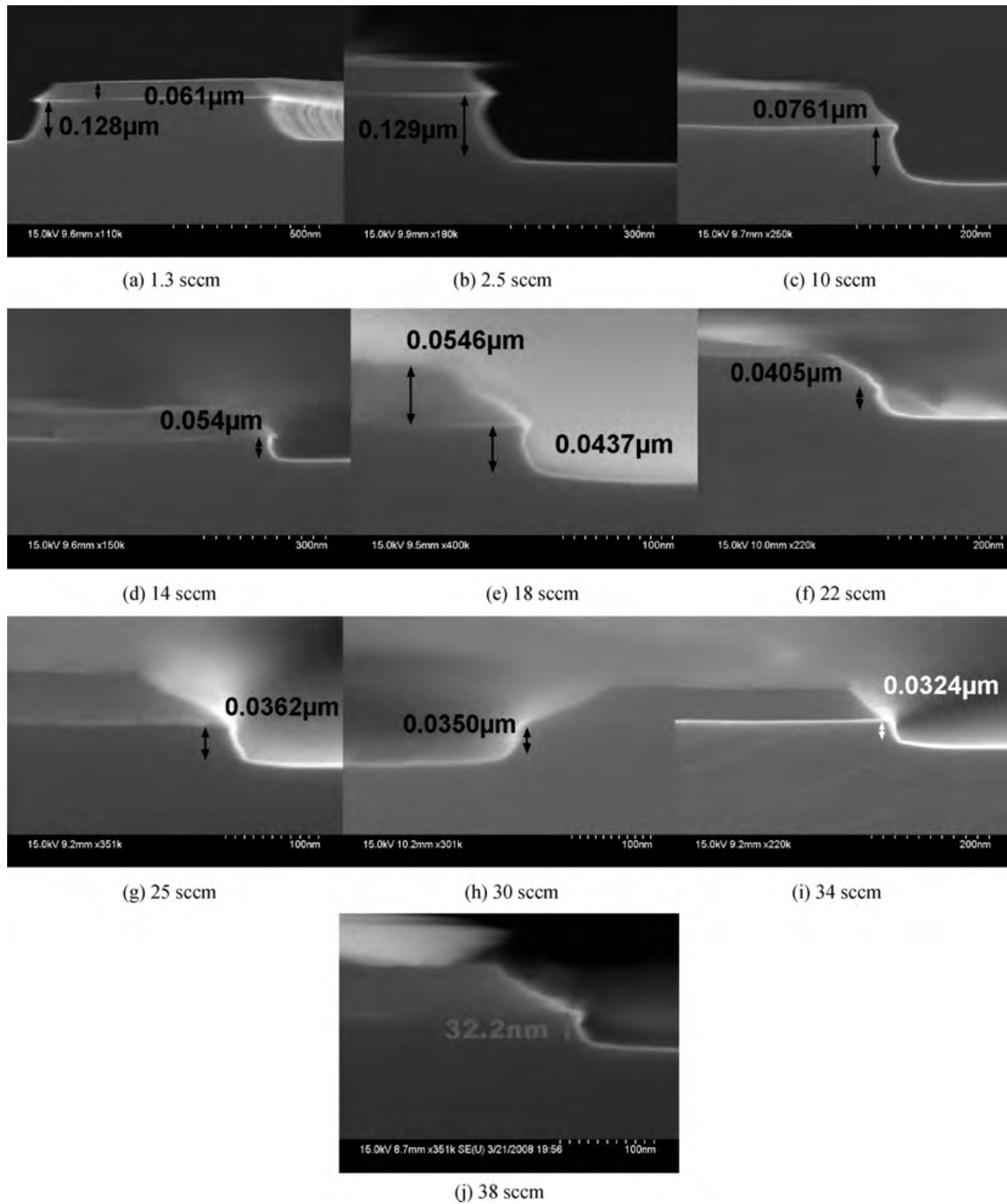

Fig. 2. Effect of different Ar flow rates on the etch profile at low RF power levels.

Ar flow because there is more total gas in the chamber but the $SiCl_4$ is more dilute. As a result, we found the optimal Ar flow region was 18–34 sccm and we can find a suitable etching rate and etching profile in this region.

4. Etching damage evaluation

A major advantage expected from our slow etching process is that there should be minimal damage to the active layers below due to the low RF power used in the etch. To investigate this, we carried out photoluminescence (PL) measurements and compared the peak position, peak intensity and full width at half maximum (FWHM) before and after our slow etching process.

The epi structure of the sample is shown in Fig. 4(a). All layers except the substrate are undoped. First, the GaAs cap layer and the upper AlGaAs cladding layer were selectively removed with a wet etch. Then, the wafer was cleaved into several samples. Next, we applied our dry etch process on the upper GaAs core with the parameters: RF1 at 10 W, RF2 at 20 W, $SiCl_4$ flow at 1sccm, and Ar flow at 34 sccm and the etching times for the samples were 0, 1, 3, 5 and 7 min, respectively. The etching rate was 16 nm/min and so the remaining GaAs thicknesses were approximately 130, 114, 82, 50 and 18 nm, respectively.

Figure 4(b) shows the PL spectra of the samples before and after dry etching. The etching does not cause significant material degradation. Each spectrum has its peak position within 0.2 nm of 976.6 nm. This variation is negligible when compared to the 0.2 nm step size of the PL instrument as well as the non-uniformity in PL peak across the unetched wafer. The 976.6 nm peak is due to the E^1–HH^1 transition, which is the lowest energy transition for the 8 nm InGaAs quantum well (QW). The peak near 929 nm is attributed to the E^1–LH^1 and/or the

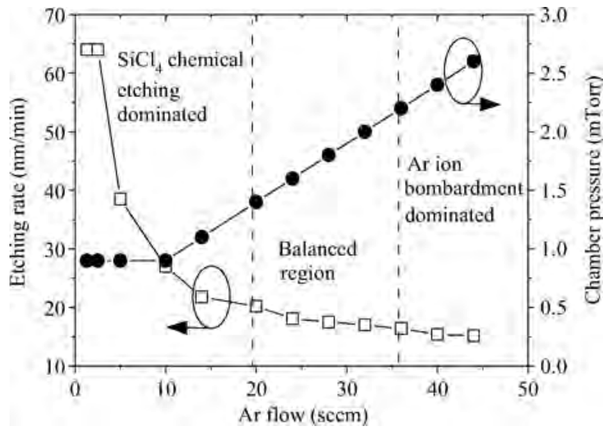

Fig. 3. Etching rate and chamber pressure as a function of Ar flow.

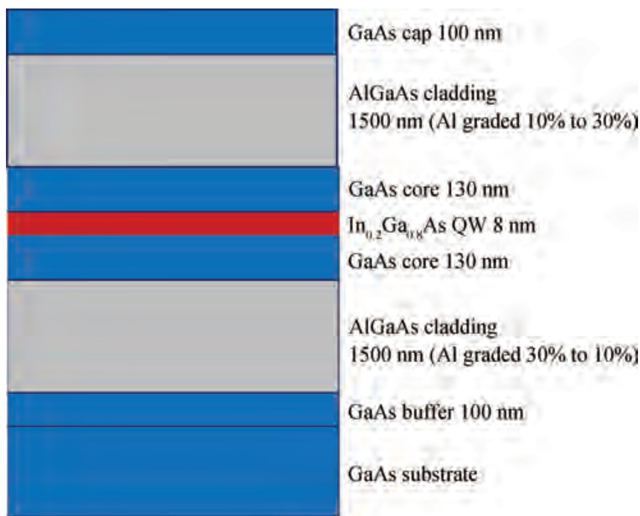

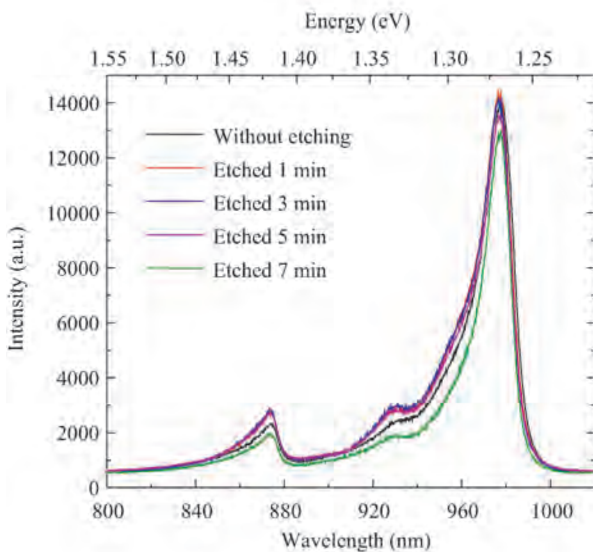

Fig. 4. (a) Epitaxial structure of test sample. (b) PL spectra before and after etching.

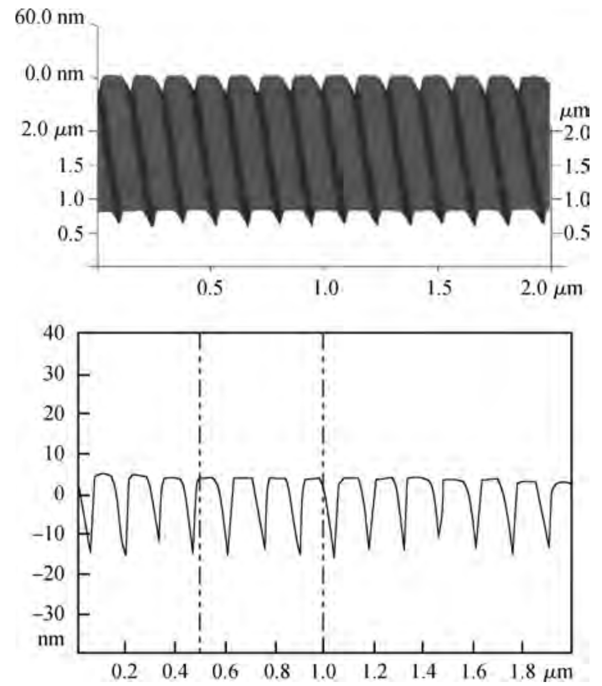

Fig. 5. AFM analysis of the GaAs grating.

continuum-HH^2 transition. The excitation light from the Ar source at 488 nm is severely attenuated by the GaAs waveguide core and AlGaAs lower cladding and does not reach the substrate. Thus, the peak at 870 nm is due to recombination in the GaAs core. The peak and integrated intensities are comparable for all etches except the deepest etch. In fact, there is a slight 3%–5% increase in integrated intensity for the 1, 3 and 5 min etched samples compared to the unetched sample. This increase is likely due to improved pumping of the quantum well because of reduced absorption in the top GaAs core. The FWHMs are 18.9, 20.0, 19.7, 19.8 and 16.1 nm (24.6, 26.2, 25.8, 25.9 and 20.9 meV), respectively. This variation is also negligible except for the narrower FWHM of the deepest etched sample. The reduced FWHM and 17% lower integrated intensity for the deepest etched sample imply that the QW carrier density is lower, especially since most of the intensity reduction is on the high energy side of the main peak. There may be several causes for this decrease in QW carrier density: (1) a lower pump intensity incident on the QW layer due to interference effects from the cavity formed by the air–GaAs and GaAs–$In_{0.2}GaAs$ interfaces ($\lambda/4n = 28$ nm); (2) an increase in the reflection into the substrate of the emitted light due to the change in the cavity above; (3) an increase in non-radiative recombination since the surface states are now much closer to the active region; or (4) deterioration of the active region itself. Nevertheless, we conclude that the damage to the active region from our dry etching process is very slight at most. Additional PL tests with a 915 nm light source, which would not be absorbed by GaAs, are planned to be able to rule out some of these effects.

5. GaAs grating fabrication

We carried out the etching process on shallow first order GaAs gratings with a period of 140 nm. The etching method

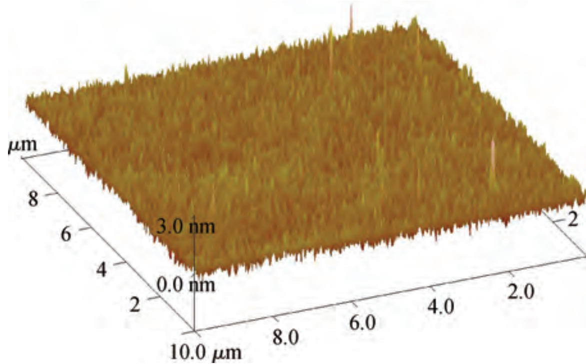

Fig. 6. 3-D morphology of an etched large area region.

was the same as in the last section. We patterned a 15 nm Ti thin film using e-beam lithography and liftoff to serve as the etching mask. Figure 5 shows the 3-D AFM picture of the etched GaAs grating after removing the Ti etching mask with a buffer oxide etchant (BOE). From the section analysis data, we can see that the etching depth was 25 nm after 2 min of etching. This is shallower than expected, because the etching rate of the calibration sample was 17 nm/min. This can be explained by the lag effect of plasma etching[15, 16], where the etching rate of the semiconductor material is influenced by the size of the etching opening. Smaller openings results in lower etching rates. The 3-D surface morphology of a large area etched region is given in Fig. 6. The RMS roughness is 0.3 nm, which is comparable to RMS roughness of epi ready GaAs wafer, and epitaxial wafer of 0.2 nm. Note that the RMS roughness of the high rate etched GaAs wafer was 1.2 nm with an etching rate of 1.3 μm/min in our previous experiments. This degree of slow etched surface smoothness enables us to regrow the upper cladding layers of distributed Bragg reflector (DBR) laser devices.

6. Conclusion

Highly controllable GaAs ICP etching with $SiCl_4$/Ar plasma was investigated in terms of RF power levels and gas flow. An etching rate as low as 13 nm/min was obtained with the optimal parameters. Shallow GaAs gratings with 25 nm depth and 140 nm period were fabricated successfully. The RMS roughness of the etched surface over a large area was 0.3 nm, which is good enough to regrow the high quality materials for device fabrication.

Acknowledgment

The authors are grateful for startup fund support from Huaqiao University.

References

[1] Granier H, Tasselli J, Marty A, et al. A SiC_4 reactive ion etching and laser reflectometry process for AlGaAs/GaAs HBT fabrication. Vacuum, 1996, 47(11): 1347

[2] Frei M R, Chiu T Y, Abernathy C R, et al. Degradation of GaAs/AlGaAs heterojunction bipolar transistors with ion-implant isolation. Solid-State Electron, 2001, 45(9): 1301

[3] Goddard L, Kallman J, Bond T, et al. Rapidly reconfigurable all-optical universal logic gates (invited). Proc SPIE, 2006, 6368(H): 1

[4] Jalabert L, Dubreuil P, Carcenac F, et al. High aspect ratio GaAs nanowires made by ICP-RIE etching using Cl_2/N_2 chemistry. Microelectron Eng, 2008, 85(5/6): 1173

[5] Li X, Cao X, Zhou H, et al. A low damage RIE process for the fabrication of compound semiconductor based transistors with sub-100 nm tungsten gates. Microelectron Eng, 2006, 83(4–9): 1159

[6] Golka S, Austerer M, Pflügl C, et al. Processing of deeply etched GaAs/AlGaAs quantum cascade lasers with grating structures. Materials Research Society Symposium Proceedings, 2005, 829(1): 245

[7] Jung M, Lee S, Jhon Y M, et al. Nanohole arrays with sub-30 nm diameter formed on GaAs using nanoporous alumina mask. Jpn J Appl Phys, 2007, 46(7A): 4410

[8] Dultsev F, Nenasheva L. The effect of hydrogen as an additive in reactive ion etching of GaAs for obtaining polished surface. Appl Surf Sci, 2006, 253(3): 1287

[9] Maher H, Etrillard J, Decobert J, et al. Dry etch recess of an InGaAs/InAlAs/InP HEMT like structure using a low energy high density $SiCl_4$ plasma. Indium Phosphide and Related Materials Conference, 1998, 1(1): 793

[10] Schartner S, Golka S, Pflügl C, et al. Deeply etched waveguide structures for quantum cascade lasers. Microelectron Eng, 2006, 83(4–9): 1163

[11] Etrillard J, Ossart P, Patriarche G, et al. Anisotropic etching of InP with low sidewall and surface induced damage in inductively coupled plasma etching using $SiCl_4$. Journal of Vacuum Science and Technology A, 1997, 15(3): 626

[12] Lee H W, Kim M, Min N K, et al. Etching characteristics and mechanism of InP in inductively coupled HBr/Ar plasma. Jpn J Appl Phys, 2008, 47(8): 6917

[13] Yoon S F, Ng T K, Zheng H Q. Study of GaAs and GaInP etching in Cl_2/Ar electron cyclotron resonance plasma. Thin Solid Films, 2001, 394(1/2): 249

[14] Nam P S, Ferreira L M, Lee T Y, et al. Study of grass formation in GaAs backside via etching using inductively coupled plasma system. J Vac Sci Technol B, 2000, 18(6): 2780

[15] Chung C K. Geometrical pattern effect on silicon deep etching by an inductively coupled plasma system. J Micromechan Microeng, 2004, 14(4): 656

[16] Akimoto T, Nanbu H, Ikawa E. Reactive ion etching lag on high rate oxide etching using high density plasma. J Vac Sci Technol B, 1995, 13(6): 2390